ARTICLE NO. 78-1485R

Drones for Aerodynamic and Structural Testing (DAST) — A Status Report

H. N. Murrow* and C. V. Eckstrom†
NASA Langley Research Center, Hampton, Va.

A program for providing research data on aerodynamic loads and active control systems on wings with supercritical airfoils in the transonic speed range is described. Analytical development, wind-tunnel tests, and flight tests are included. A Firebee II target drone vehicle has been modified for use as a flight test facility. The program currently includes flight experiments on two aeroelastic research wings. The primary purpose of the first flight experiment is to demonstrate an active control system for flutter suppression on a transport-type wing. Design and fabrication of the wing are complete and, after installing research instrumentation and the flutter suppression system, flight testing is expected to begin in August 1979. The experiment on the second research wing—a fuel-conservative transport-type—is to demonstrate multiple active control systems, including flutter suppression, maneuver load alleviation, gust load alleviation, and reduced static stability. Of special importance for this second experiment is the development and validation of integrated design methods which include the benefits of active controls in the structural design.

I. Introduction

CORRELATION of theoretical and experimental results is a traditional method for assessing advanced design technology. The methods used in testing nearly always are a compromise between the ideal and the practical. This situation is especially true for tests of aeroelastic models. Wind-tunnel tests in the transonic range are traditionally limited by model size, dynamic pressure (for aeroelastic tests), and effects of interaction between the model and reflected shock waves. Full-scale piloted flight tests are restrained by cost and considerations of safety of onboard personnel, especially for flutter tests. A recently initiated NASA program, Drones for Aerodynamic and Structural Testing (DAST), uses an unmanned target drone aircraft for special high-risk flight tests and provides a test method that is a strong complement to wind-tunnel and full-scale piloted testing. Primary focus is on tests in the transonic speed range. For this program, maneuverability requirements are minimal for the test bed vehicle; it is merely used to subject research wings to selected flight conditions. It is sometimes referred to as a flight test facility or "wind tunnel in the sky." Since the test vehicle has a parachute recovery system, retrieval is possible even in cases of structural failure. The program is primarily NASA in-house with contracted support as necessary.

The principal research objectives of the DAST program are to validate: 1) systems synthesis and analysis developments for active control of aeroelastic response and 2) analysis techniques for aerodynamic loads prediction. These objectives will be accomplished by means of experiments on selected aeroelastic research wing (ARW) configurations. Benefits of flight testing include: 1) elimination of questions concerning tunnel interference effects with walls and model mountings; 2) achievement of realistic Mach number and dynamic pressure combinations; 3) higher Reynolds numbers by factors of three to four; and 4) inclusion of inertial effects, i.e., maneuvering with associated aeroelastic effects.

The purpose of this paper is to describe the DAST program with emphasis on the flight test activity, and present a status report on activities completed, underway, and planned. The currently approved program includes flight tests of two transport-type aeroelastic research wings incorporating active control systems. Analytical studies and wind-tunnel tests are essential and included as major ingredients of the program.

II. DAST Test Vehicle and Flight Operations

The Navy-developed Firebee II recoverable target drone vehicle (Fig. 1) has been selected as the basic test bed for the program because of its size, relatively clean aerodynamic shape, performance, maneuver load capability (5 g design), and available volume for research equipment. Early loads tests on a standard Firebee II wing of aspect ratio 2.5 were conducted with the cooperation of Navy personnel at Pt. Mugu, Calif. Results of these flight tests are reported in Refs. 1-4.

A preliminary design-type study was also performed under contract[5] to define the feasibility of testing different wing configurations on the Firebee II vehicle. Wing sizes and corresponding operational envelopes were defined in this study; some results for three of the potential plan forms are shown in Fig. 2. Note that the endurance turbofan had the highest aspect ratio and a lower cruise speed than the so-called transport that would cruise at $M=0.98$. A low aspect ratio wing considered applicable for a fighter was selected to complete the scope of possibilities

DAST uses an Air Force version of the Firebee II which includes an auxiliary fuel tank, a midair retrieval system, a modified flight control system, with target equipment removed to make room for research equipment. The vehicle arrangement for research flights is shown in Fig. 3. Note the specially developed antennas which are surface-mounted on the nose section to avoid possible radio-frequency-interference that could result from the use of wing-tip-mounted stub antennas which would require cabling routed through the wing where research instrumentation is located.

The operational sequence for flight involves air launch and midair retrieval (Fig. 4). JATO-assisted ground launch capability exists, but for research tests, air launch was chosen

Presented as Paper 78-1485 at the AIAA Systems and Technology Conference, Los Angeles, Calif., Aug. 21-23, 1978; submitted Aug. 31, 1978; revision received Jan. 26, 1979.

Index categories: Structural Design (including Loads); Testing, Flight and Ground; Structural Dynamics.

*Aerospace Engineer. Associate Fellow AIAA.
†Aerospace Engineer. Member AIAA.

Fig. 1 Firebee II target drone in flight.

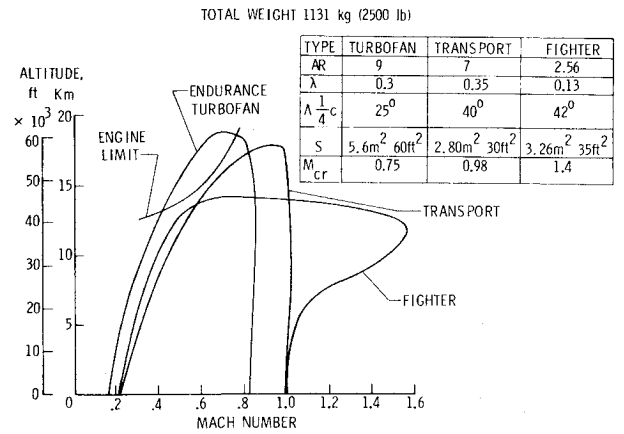

Fig. 2 Operational envelopes and wing sizes for three candidate configurations.

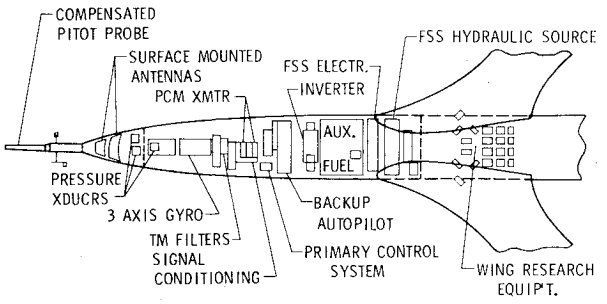

Fig. 3 Equipment arrangement for DAST research flights.

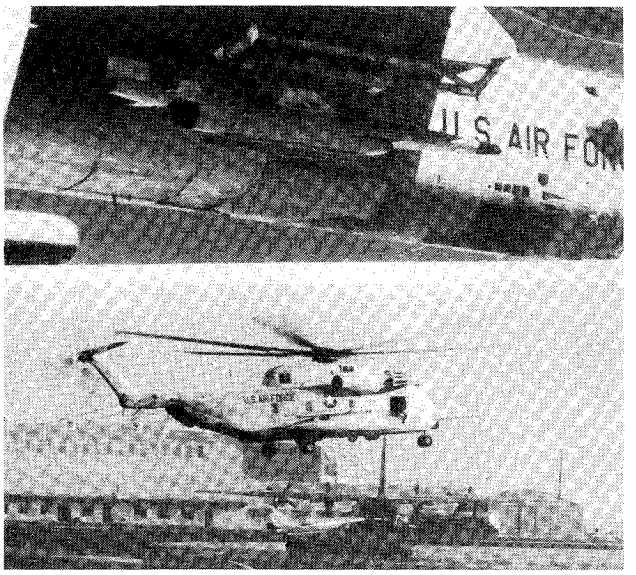

Fig. 4 Launch and recovery methods for DAST flights.

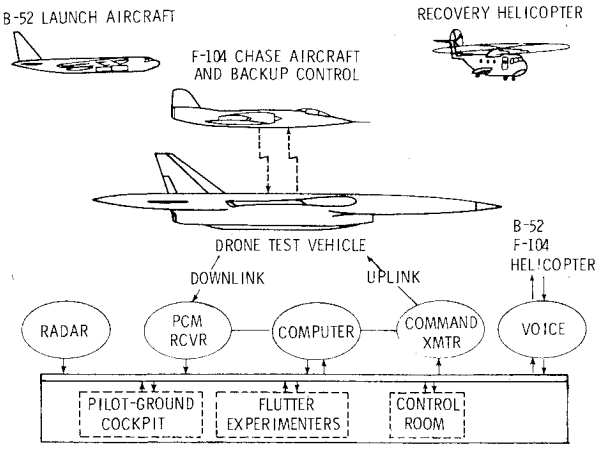

Fig. 5 Elements involved in a DAST flight test operation.

because it allows for more test time and is believed to be safer. Landing gear or skids could be developed, but because of cost and integration difficulties, this option has not been pursued to date.

The drone vehicle was designed as a target, and the engine design does not allow for a reduction of power to less than that corresponding to 80% of the maximum rpm value without danger of a flameout. Therefore, the minimum flight speed at most altitudes is limited by the minimum allowable throttle setting rather than by aircraft stall, which is more usually the case. The available speed range is adequate for some test configurations; however, some form of drag enhancement such as speed brakes will probably be required for achieving desired test conditions for other configurations.

The flight testing will be conducted by NASA personnel at the Dryden Flight Research Center located at Edwards AFB, Calif. Overall test philosophy is probably more similar to rocket flight tests than traditional aircraft flight tests in that only a minimal number of flights are planned (6-8 flights). Significant support is required for each test, and the operational setup is similar to that used in an earlier program for unpowered remote piloted spin tests as described in Ref. 6. The elements of a DAST flight test operation are depicted in Fig. 5.

A B-52 aircraft, which includes vehicle system checkout and engine starting equipment and provides continual fuel top-off up until release of the test vehicle, is used as the carrier and launch vehicle. An F-104 provides normal chase aircraft coverage and is equipped to command the test vehicle to recovery through a backup mode in case of malfunction of the primary command control system. Data are provided by means of pulse-code-modulated (PCM) telemetry transmission, and a test pilot controls the vehicle from a ground cockpit equipped with necessary displays. Experimenters provide real-time assessment of the status of the research wing and associated active control systems. Specially equipped Air Force helicopters with AF crews experienced in midair recovery are brought in for each flight to provide retrieval. Flight tests on the first research wing are expected to begin in August 1979.

III. First Research Wing

The first research wing selected for study and flight test (referred to as ARW-1 for aeroelastic research wing 1) has an aspect ratio of 6.8 and a supercritical airfoil designed for cruise at $M=0.98$. Wind-tunnel and flight tests had already been conducted with this wing configuration[7,8] prior to its selection for further study here. The wing structure was designed under contract‡ and fabricated in NASA Langley experimental shop facilities. The wing was designed for a maneuver limit load of 2.5 g, and was purposely designed to flutter within the operating envelope of the flight con-

‡Teledyne-Ryan Aeronautical, San Diego, Calif.

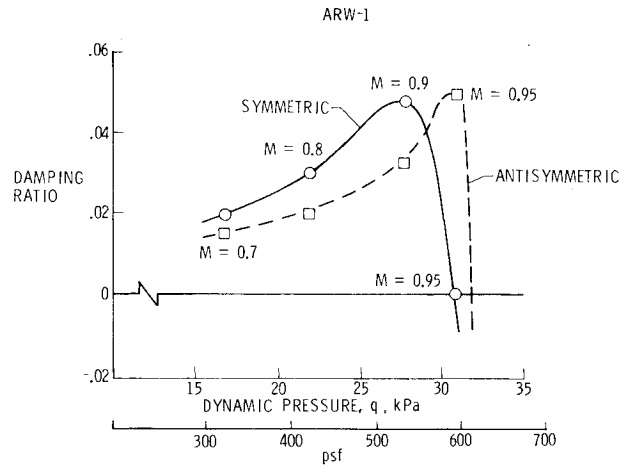

Fig. 6 Predicted flutter onset at 6.1 km altitude.

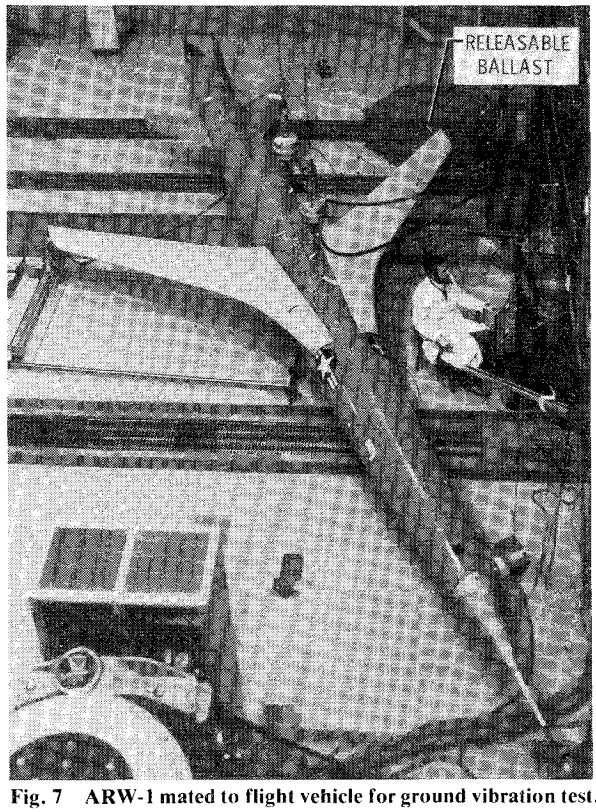

Fig. 7 ARW-1 mated to flight vehicle for ground vibration test.

figuration. To achieve this behavior, reduced torsional stiffness was achieved through the use of wing skins fabricated of fiberglass. The fiberglass filaments were laid parallel and perpendicular to the wing front spar; thus, the torsional stiffness is essentially the stiffness of the binder material (matrix). In most instances, design (handbook) values of material properties are close to, but slightly less than, actual properties, i.e., conservative. This situation resulted in a fabrication problem with respect to the fiberglass material used for the ARW-1 wing skin surfaces. When skin sample coupons had been fabricated and tested, it was found that the fiberglass material torsional modulus quoted in MIL-HDBK-17 turned out to be understated or conservative by about 50%. The wing torsional stiffness was, therefore, much greater than anticipated, and the wing was flutter-free over a larger portion of the flight envelope than acceptable for the research tests. To resolve this problem and overcome the increased wing torsional stiffness, the wing was unbalanced by adding ballast masses aft of the trailing edge.

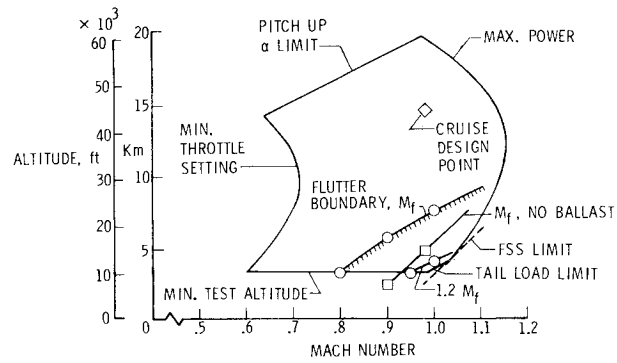

Fig. 8 Flight envelope and flutter boundaries for ARW-1.

The primary flutter modes result from combined bending and torsion and Fig. 6, which presents predicted damping ratio vs dynamic pressure for both the symmetric and antisymmetric flutter modes, indicates that flutter has an explosive onset, and that the symmetric and antisymmetric modes become unstable at about the same flight condition. Corresponding Mach numbers are indicated at each calculated data point on Fig. 6. The wing is shown mated to a Firebee II vehicle in Fig. 7. The ballast masses mounted aft of the trailing edge near the wing tip (note Fig. 7) are used to adjust the basic flutter boundary to the desired condition. As a safety feature, the ballast masses are ejectable by means of an automatic release feature, such that they are released when the wing tip acceleration reaches a preset value. Release of the ballast immediately causes the wing to be flutter-free up to a significantly higher dynamic pressure.

The flight envelope for the vehicle with the ARW-1 wing including significant boundaries is shown in Fig. 8. Performance data are based on results obtained from wind-tunnel tests of a one-sixth scale force model. Stability data obtained from the force model tests were used to develop the vehicle flight control system. The maximum power limit indicates the level flight performance boundary at full throttle. This wing exhibits a pitch-up tendency at angles of attack greater than about 6 deg, which, in this case, will be avoided by α-limiting in the flight control system. The minimum throttle setting for the YJ69-T-406 engine determines the boundary at the left of Fig. 8. For safety purposes, including recovery aspects, tests will not be conducted below 10 kft (3.05 km) altitude. This overall envelope is truncated slightly at the highest dynamic pressure (lower right-hand corner) by the limit load on the horizontal tail. The predicted basic flutter boundary (M_f) for the wing and the flutter boundary after ballast ejection are indicated.

An active control system for flutter suppression has been designed, fabricated,§ and installed in the wing. Results from a preliminary design study are given in Ref. 9. The primary purpose of flight tests of the wing is to verify transonic flutter prediction techniques and to validate predicted flutter suppression system (FSS) performance. A goal of the tests is to demonstrate that this active control system for flutter suppression can provide a 20% increase in the flutter velocity boundary. Surface pressures and total loads on the wing will also be measured. The 1.2 M_f boundary is also shown on Fig. 8. The predicted operational limit of the flutter suppression system is shown by the dashed line at the far right. The demonstration of 20% increase was selected, based on indications that the first use of FSS on commercial transports will probably be to satisfy design criteria that the airplane be flutter-free to 20% above the flight envelope; thus, the system would only be required to operate if the airplane exceeded the planned operational envelope. References 9-11 describe some

§The Boeing Co., Wichita, Kansas

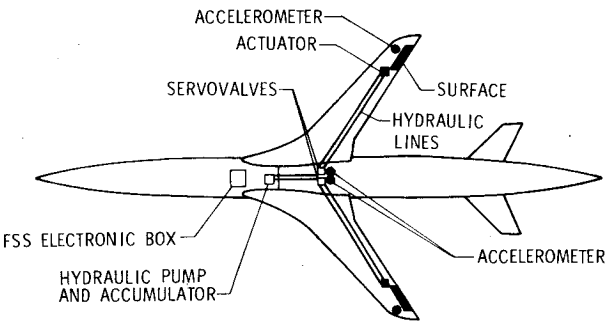

Fig. 9 Sketch of ARW-1 flutter suppression system installation.

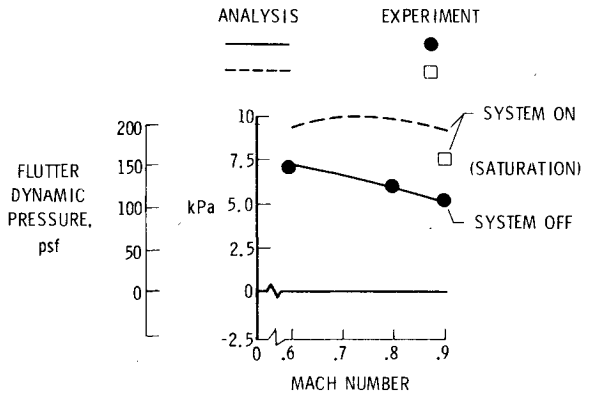

Fig. 10 Wind-tunnel results for aeroelastic model of ARW-1 with FSS on and off.

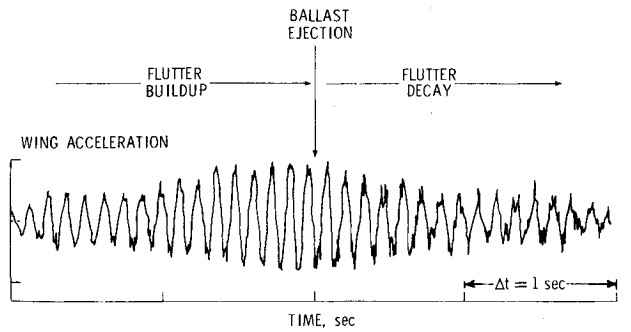

Fig. 11 Wind-tunnel demonstration of effectiveness of ballast release.

of the synthesis, design, and analysis efforts for the FSS. The basic components of the active control system are shown on Fig. 9.

For purposes of assessing analysis adequacy and gaining some experience with the system, a dynamically (frequency) scaled aeroelastic wind-tunnel model with the same control surface and basically the same control law was fabricated and tested in the NASA Langley 16-ft Transonic Dynamics Tunnel. Results correlated well with prediction for system-off as seen in Fig. 10. The system saturated (limit cycled), however, at a velocity 19% (dynamic pressure of 42%) beyond the system-off flutter boundary, which is slightly less than the planned demonstration goal of 20% margin in velocity (44% in dynamic pressure), and significantly less than the predicted system-on flutter limit. Saturation was attributed to the turbulence in the tunnel which is significantly higher than expected in the atmosphere. Another problem encountered involved interference of high-frequency modes with FSS operation. The problem was believed to be associated with the interaction of the hydraulic system installation and the structure and was evident with wind-off systems tests. The addition of filters solved this problem. It is

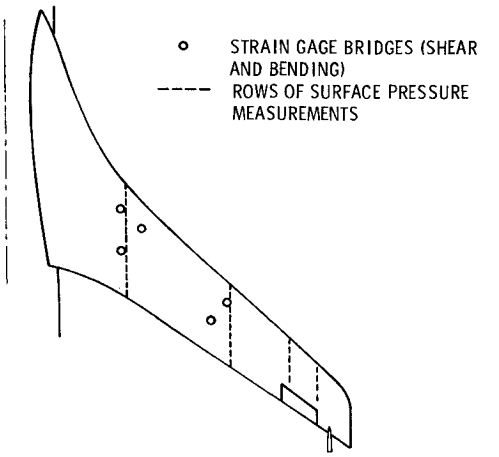

Fig. 12 Location of sensors for aerodynamic loads measurements.

planned that ground tests of the flight system will include investigation of stability at high gain (~2.) to identify any similar problem, if it exists.

A demonstration of the ballast release effectiveness as a "flutter stopper" was also made during the wind-tunnel test series. The flutter suppression system was turned off with the dynamic pressure just above the flutter boundary, and the acceleration at the wing tip was allowed to increase as indicated by the time history in Fig. 11. The ballast was then ejected and a decrease in amplitude was evident in the next cycle of oscillation; 2 s later the amplitude was reduced to about one-third the peak value.

Analysis indicates that flutter buildup would be so rapid after deep penetration into the flutter region in flight that the ballast release would most likely not prevent destruction of the wing. Under present plans, however, nearly all the testing will be in the vicinity of the flutter boundary. One flight test will be devoted to demonstrating the 20% velocity margin referred to earlier.

A secondary objective of the flight test series for this wing is to obtain aerodynamic loads measurements over a range of Mach number from about 0.65-0.98 and dynamic pressure from 7 to above 28 kPa (150-600 psf) in straight-and-level and maneuvering (up to 2.5 g) flight. As shown on Fig. 12, the wing is instrumented to measure surface pressures at four spanwise locations. In addition, strain gage bridges calibrated to provide shear, bending moment, and torsional moment are included. A camera package has also been designed to provide measurements of wing deformations in flight. The camera will be housed in a pod mounted on the keel along the centerline underneath the fuselage and will focus on targets painted on the lower surface of the wing. Data from the instrumentation just described will be used to evaluate mathematical models, jig-shape determination, and to assess latest programs for computing steady-state transonic pressure distributions.

The photograph of Fig. 7 was taken during the ground vibration test series where mode shapes and frequencies were measured. It was determined that differences between the full-fuel and fuel-empty conditions were negligible with regard to mode shape and frequency. All fuel is located within the

Table 1 Frequency comparisons for symmetric modes

Mode	Frequency, Hz	
	Analysis	Measured
Wing first bending	9.1	9.8
Fuselage first bending	16.4	16.6
Wing second bending	29.9	30.9
Wing first torsion	48.8	49.2

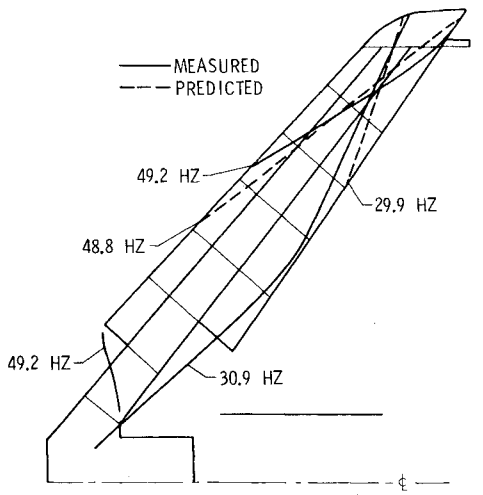

Fig. 13 Comparison of measured and predicted node lines.

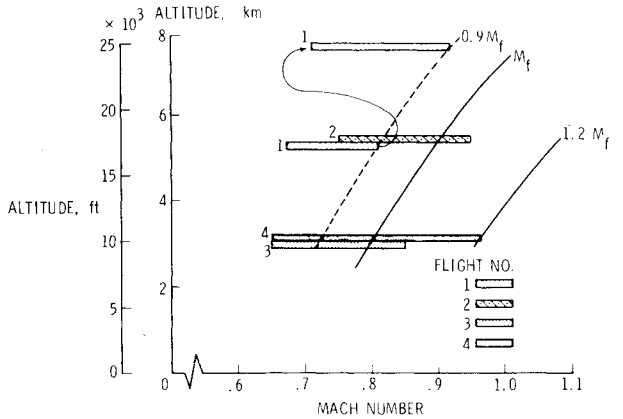

Fig. 14 Planned flight test sequence.

fuselage with the main tank centered on the center of gravity. A comparison between the measured second symmetric wing bending and torsion node lines and those predicted by analysis of a NASTRAN structural mathematical model are shown in Fig. 13. Frequency comparisons for the four most significant symmetric modes are shown in Table 1.

IV. Test Planning for ARW-1

The planned six-flight flutter test sequence is described in reference to Fig. 14. An intermediate altitude will be selected and data will be obtained at approximately 0.05 increments of increasing Mach number (approximately 1% increments in engine rpm). The wing will be excited at each data point by commanding an onboard function generator to drive the active control surfaces. Excitation will include frequency sweeps and pulses, both symmetric and antisymmetric. The first flight will be aimed at evaluating the active control system operation at medium and high altitudes in the presence of significant dynamic pressure and, if possible, to estimate from subcritical response measurements the expected Mach number where flutter will be encountered. The flutter boundary is to be exceeded on the second flight with the FSS on. On the third flight, the FSS will remain off until flutter onset is evident; at this point, the FSS will be turned on and the boundary exceeded by some arbitrary increment. On the fourth flight, at low altitude, the main objective will be to demonstrate that the system is indeed capable of providing a 20% increase in the flutter Mach number. It is expected that at least two additional flights will be needed to satisfy remaining questions.

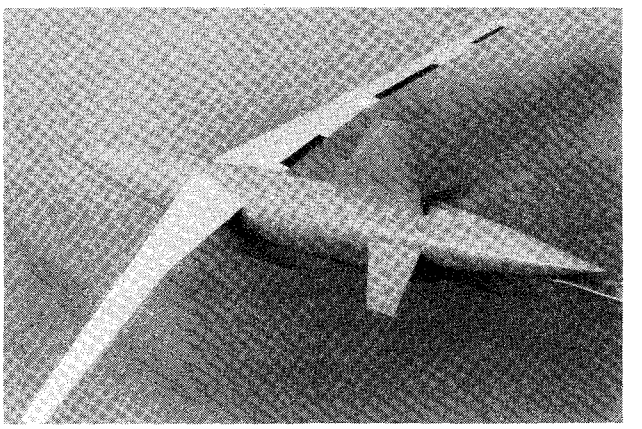

Fig. 15 Wind-tunnel force model of ARW-2 configuration.

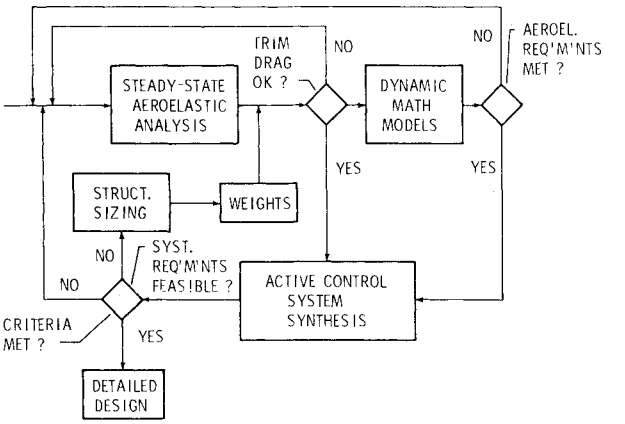

Fig. 16 Iterative design loop applied to ARW-2.

V. Second Research Wing

The second research wing (ARW-2) provides a focus for studies on the benefits and applicability of multiple-active controls for a fuel-conservative transport-type wing. This wing has a supercritical airfoil designed for cruise at $M = 0.8$, with an aspect ratio of 10.3 and a midchord sweep angle of 25 deg. A photograph of a wind-tunnel force model of the overall configuration is given in Fig. 15. Hinge moments were also measured on the candidate active control surfaces shown in the photograph. Active control systems for flutter suppression, gust load alleviation (GLA), and maneuver load alleviation (MLA) are mandatory for the flight of this wing within the operational envelope; for example, the wing is not capable of maneuvering to the 2.5 g design value without the maneuver control system operating. Relaxed static stability is included in the overall system primarily in order to include any possible effects of interference between the various control systems.

The development of an iterative design procedure combining aerodynamics, structures, and control system disciplines that allow the structural design to fully reflect the benefits provided by the active control systems is of special interest. Compatible mathematical models for the different disciplines is important. The design loop selected for the ARW-2 design is shown in Fig. 16. The inclusion of the active control system synthesis block requires that additional criteria be satisfied prior to proceeding into detailed design. Application of gust and maneuver load alleviation yielded about 20% reduction in wing root bending moment for this wing. A comparison of effects of GLA relative to MLA should be made on a regular basis in the design process since, obviously, there is no advantage in reducing one of these loadings significantly below the other from a design load standpoint.

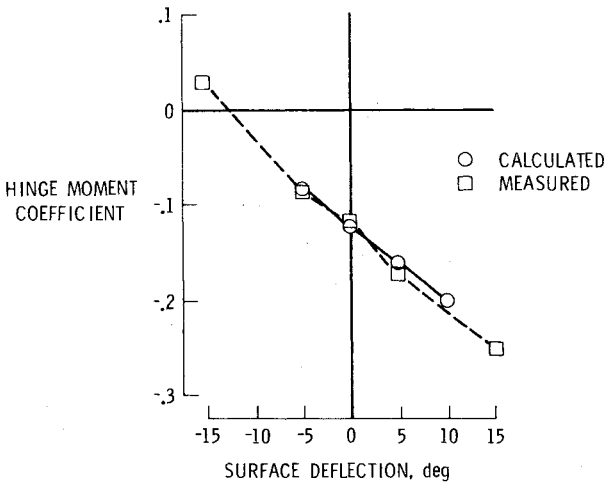

Fig. 17 Comparison of calculated and measured hinge moment coefficients for ARW-2.

CONTROL SURFACE	SIZE % CHORD	% SEMISPAN
1	15	15.8
2	15	10.5
3	23	15.8

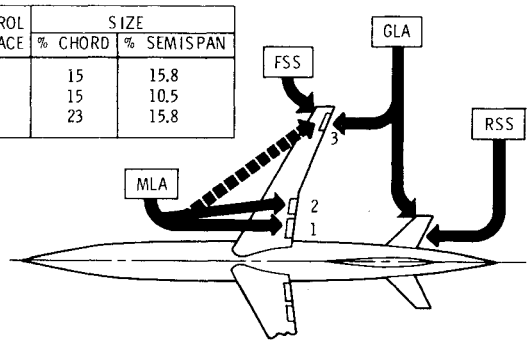

Fig. 18 Control surface locations and functions for ARW-2.

Fatigue considerations are not included in this particular exercise.

The added complication of dealing with a supercritical airfoil resulted in the development of a method for predicting steady-state loads using a boundary-layer program in conjunction with a three-dimensional transonic computation program;[12] this method was also applied to predict control surface hinge moments.[13] As shown in Fig. 17, analytical predictions of hinge moment compared well with wind-tunnel measurements.

The design process has led to control surface locations, sizes, and utilization as shown on Fig. 18. The primary maneuver load alleviation control law utilizes control stick movement as a sensor to activate the system. Gust load alleviation depends on sensing by an accelerometer at the center of gravity and, at low frequency, the GLA system also provides some maneuver load alleviation from the outboard control surface. This situation is indicated by the dashed line for MLA on Fig. 18.

A rather elaborate wind-tunnel rigid semispan wing model is nearing completion for parametric research studies of fluctuating pressures associated with oscillating (active) control surfaces and measurements of dynamic hinge moments. This model of aspect ratio 10.76 has a 90-in. semispan and five leading edge and five trailing edge control surfaces. The actuators are capable of providing surface deflections of ±15 deg with frequency response flat to 30 Hz. A total of 234 pressure orifices are provided, with 164 of these attached to dynamic pressure transducers. Results from tests of this model, which will be conducted in the Langley Transonic Dynamics Tunnel, should be especially helpful for active control systems design in general, in addition to being applicable for ARW-2 analyses.

Measurements will be made of the ARW-2 wing deformations in flight using the technique described earlier, and load-measuring sensors (pressure transducers and calibrated strain gage bridges) will measure load distribution and alleviation provided by the active control systems. Some flights must be made in turbulence to evaluate the gust load alleviation system. The program is being phased such that flight testing of this research wing is planned to begin within a year after completion of tests on the ARW-1.

VI. Concluding Remarks

A status review has been given for a program focused on analytical and experimental studies of aeroelastic effects on loads and the use of active controls for load alleviation and flutter suppression. Early studies involve supercritical transport-type wings in the transonic region. Flight tests of a high risk nature will be conducted in a realistic flight regime using a modified target drone vehicle as a test bed, primarily to validate design and analysis methods. Analytical developments and wind-tunnel tests are key elements in the program. It is believed that successful completion of this program will enhance acceptance and utilization of active control systems in future transports including fuel-conservative designs.

References

[1] Peele, E.L. and Eckstrom, C.V., "Strain-Gage Bridge Calibration and Flight Loads Measurements on a Low-Aspect-Ratio Thin Wing," NASA TN D-7979, 1975.

[2] Eckstrom, C.V. and Peele, E.L., "Flight Assessment of a Large Supersonic Drone Aircraft for Research Use," NASA TM X-3259, 1975.

[3] Eckstrom, C.V., "Flight Loads Measurements Obtained from Calibrated Strain-Gage Bridges Mounted Externally on the Skin of a Low-Aspect-Ratio Wing," NASA TN D-8349, 1976.

[4] Byrdsong, T.A., "Flight Measurements of Lifting Pressures for a Thin Low-Aspect-Ratio Wing at Subsonic, Transonic, and Low Supersonic Speeds," NASA TM X-3405, 1977.

[5] James, H.A., "Feasibility Study of Modifications to BQM-34E Drone for NASA Research Applications," NASA CR-112323, 1972.

[6] Edwards, J.W. and Deets, D.A., "Development of a Remote Digital Augmentation System and Application to a Remotely Piloted Research Vehicle," NASA TN D-7941, April 1975.

[7] Bartlett, D.W. and Harris, C.D., "Aerodynamic Characteristics of a NASA Supercritical-Wing Research Airplane Model With and Without Fuselage Area-Rule Additions at Mach 0.25 to 1.00," NASA TM X-2633, 1972.

[8] "Supercritical Wing Technology—A Progress Report on Flight Evaluations," NASA SP-301, 1972.

[9] Visor, O.W. and Sevart, F.D., "Preliminary Design Study of Flutter Suppression Control System for BQM-34E/F Drone Aircraft with a Supercritical Wing—Final Report," NASA CR 145208, 1976.

[10] Abel, I., Perry III, B., and Murrow, H., "Synthesis of Active Controls for Flutter Suppression on a Flight Research Wing," *Journal of Guidance and Control*, Vol. 1, Sept.-Oct. 1978, pp. 340-346; also AIAA Paper 77-1062, Hollywood, Fla., Aug. 1977.

[11] Nissim, E. and Abel, I., "Development and Application of an Optimization Procedure for Flutter Suppression Using the Aerodynamic Energy Concept," NASA TP 1137, 1978.

[12] Newman, P.A., Carter, J.E., and Davis, R.M., "Interaction of a Two-Dimensional Strip Boundary Layer With a Three-Dimensional Transonic Swept-Wing Code," NASA TM-78640, 1978.

[13] Perry III, B., "Control-Surface Hinge-Moment Calculations for a High-Aspect-Ratio Supercritical Wing," NASA TM-78664, 1978.